Retinotopy versus Face Selectivity in Macaque Visual Cortex

Reza Rajimehr[1,2], Natalia Y. Bilenko[1], Wim Vanduffel[1,3], and Roger B. H. Tootell[1]

Abstract

■ Retinotopic organization is a ubiquitous property of lower-tier visual cortical areas in human and nonhuman primates. In macaque visual cortex, the retinotopic maps extend to higher-order areas in the ventral visual pathway, including area TEO in the inferior temporal (IT) cortex. Distinct regions within IT cortex are also selective to specific object categories such as faces. Here we tested the topographic relationship between retinotopic maps and face-selective patches in macaque visual cortex using high-resolution fMRI and retinotopic face stimuli. Distinct subregions within face-selective patches showed either (1) a coarse retinotopic map of eccentricity and polar angle, (2) a retinotopic bias to a specific location of visual field, or (3) nonretinotopic selectivity. In general, regions along the lateral convexity of IT cortex showed more overlap between retinotopic maps and face selectivity, compared with regions within the STS. Thus, face patches in macaques can be subdivided into smaller patches with distinguishable retinotopic properties. ■

INTRODUCTION

Visual cortical areas are typically defined on the basis of differences in histology (cytoarchitecture and myeloarchitecture), anatomical connections, functional properties, and retinotopic organization (Felleman & Van Essen, 1991). In early visual areas (e.g., V1, V2, V3), the retinotopic maps can be reliably used to distinguish the borders between areas (Fize et al., 2003; Brewer, Press, Logothetis, & Wandell, 2002; DeYoe et al., 1996; Sereno et al., 1995; Engel et al., 1994; Gattass, Sousa, & Gross, 1988). However, the retinotopic borders are less clear at progressively higher stages of the ventral visual pathway (Kravitz, Vinson, & Baker, 2008). An earlier proposal suggested that the inferior temporal (IT) cortex in macaque monkeys includes a retinotopically organized area TEO, plus nonretinotopic areas in TE (Boussaoud, Desimone, & Ungerleider, 1991; Ungerleider & Desimone, 1986). Recent fMRI studies have confirmed retinotopy and coding of position in posterior IT cortex in humans, perhaps corresponding to area TEO in macaques (Carlson, Hogendoorn, Fonteijn, & Verstraten, 2011; Cichy, Chen, & Haynes, 2011; Kravitz, Kriegeskorte, & Baker, 2010; Strother, Aldcroft, Lavell, & Vilis, 2010; Arcaro, McMains, Singer, & Kastner, 2009; Sayres & Grill-Spector, 2008; Schwarzlose, Swisher, Dang, & Kanwisher, 2008; Larsson & Heeger, 2006; Brewer, Liu, Wade, & Wandell, 2005). However, the lack of positional information in TE has been recently challenged by the demonstration of small receptive fields in anterior IT cortex (DiCarlo & Maunsell, 2003; Op De Beeck & Vogels, 2000).

How do the retinotopic maps in IT cortex relate to the functionally defined category-selective areas? Neuroimaging studies in human and macaque have reported that distinct regions in IT cortex are selective to specific object categories such as faces (e.g., Tsao, Freiwald, Knutsen, Mandeville, & Tootell, 2003; Kanwisher, McDermott, & Chun, 1997). Malach and colleagues (Hasson, Harel, Levy, & Malach, 2003; Malach, Levy, & Hasson, 2002; Levy, Hasson, Avidan, Hendler, & Malach, 2001) tested the relationship between retinotopic maps and face-selective areas in human visual cortex and reported a foveal bias in these areas (relative to a peripheral bias in the adjacent place-selective areas)—although not an explicit retinotopic map. However, the spatial resolution of fMRI images was low in those studies, and it is well known that fine-scale retinotopic details are blurred in low-resolution maps (see Discussion).

Recent fMRI studies in humans have reported a detailed retinotopic organization in "object-selective" lateral occipital cortex (Sayres & Grill-Spector, 2008; Larsson & Heeger, 2006), "scene-selective" parahippocampal cortex (Arcaro et al., 2009), and "body-selective" regions (Porat, Pertzov, & Zohary, 2011; Weiner & Grill-Spector, 2011). However, there has been no evidence for a detailed retinotopy in human face-selective area FFA, and the current literature has emphasized only on a distributed representation of positional information in this area (e.g., Schwarzlose et al., 2008).

[1]Harvard Medical School, [2]Massachusetts Institute of Technology, [3]K.U. Leuven Medical School

Journal of Cognitive Neuroscience 26:12, pp. 2691–2700
doi:10.1162/jocn_a_00672

Despite numerous studies in humans, the relationship between retinotopy and category selectivity has not yet been tested in other species. Such tests would have important implications for cross-species comparison of category-selective areas (see Discussion). Here we used high-resolution fMRI and face-based retinotopic stimuli to test the topographic relationship between retinotopic maps and face-selective patches in awake macaques. The results suggest that retinotopy is not an "all-or-none" property in the face patches. In fact, face-selective patches in IT and frontal cortex contain topographically distinct subregions, each with a specific retinotopic property. The retinotopic subregions of the face patches could be involved in coding the spatial location of faces.

METHODS

Subjects

Two juvenile (4–6 kg) male rhesus monkeys (*Macaca mulatta*) were tested in fMRI experiments. Surgical details and the training procedure for monkeys have been described elsewhere (Tsao et al., 2003; Vanduffel et al., 2001). All experimental procedures conformed to NIH guidelines and were approved by Massachusetts General Hospital animal protocols.

Imaging Procedures

Monkeys were scanned in a 3T horizontal bore magnet (Siemens Allegra, Malvern, PA). A radial surface coil (11 cm diameter) and gradient-echo EPI sequence were used for functional imaging (repetition time = 3000 msec, echo time = 24 msec, flip angle 90°, 1.25 mm isotropic voxels, and 45 coronal slices). To increase fMRI sensitivity in the awake monkey scans (to compensate for smaller voxels), we used an exogenous contrast agent (MION; 8–10 mg/kg iv). Relative to conventional BOLD imaging at 3T, the MION imaging triples the contrast/noise ratio and gives better localization within the gray matter (Leite et al., 2002; Vanduffel et al., 2001). A 3-D MP-RAGE sequence (0.35 mm isotropic voxels) was also used for high-resolution anatomical imaging while the monkeys were anesthetized.

Throughout the functional scans, subjects continuously fixated a small fixation spot at the center of a stimulus screen. Eye position was monitored using an infrared pupil tracking system (ISCAN, Woburn, MA) at 120 Hz. Monkeys were rewarded for maintaining fixation within a small central fixation window. Only scans with high behavioral performance (i.e., >90% fixation stability) were considered for statistical analysis. To increase the statistical sensitivity, each monkey was scanned in five fMRI sessions, with each session containing ~25 functional scans. Each scan consisted of 14 blocks (block duration = 30 sec).

Data Analysis

Functional and anatomical data were preprocessed and analyzed using FreeSurfer and FS-FAST (surfer.nmr.mgh.harvard.edu/). For each subject, the inflated cortical surfaces were reconstructed based on anatomical images. All functional images were motion-corrected, spatially smoothed using a 3-D Gaussian kernel (1 mm HWHM), and normalized across scans. The estimated hemodynamic response was defined by a γ function, and then the average signal intensity maps were calculated for each stimulus condition. Voxel-wise statistical tests were conducted by computing contrasts based on a univariate general linear model. To avoid sampling gaps in the (high-resolution) monkey fMRI, we averaged the functional activities from all voxels located within the gray matter along the surface normal. To optimally visualize and measure the cortical representations, the significance levels were projected onto the inflated cortex after a rigid coregistration of functional and anatomical volumes. In each monkey, the functional maps were spatially normalized across scan sessions using a spherical transformation and then averaged using a fixed-effects model.

For the ROI analysis, all voxels within a given face patch were labeled based on a "face-versus-place" localizer, and then the average percent signal change was calculated for different retinotopic conditions in each ROI.

Visual Stimuli

Stimuli were generated on a PC (Windows XP) and presented via LCD projector (Sharp XG-P25, Osaka, Japan, 1024 × 768 pixels resolution, 60 Hz refresh rate) onto a rear-projection screen. Matlab 7.0 and Psychophysics Toolbox (psychtoolbox.org/) were used to program the visual presentation codes.

The retinotopic stimuli were based on face mosaics (naturalistic "group photographs"), which were presented within retinotopically limited apertures, on a black background (Figure 1). The retinotopic apertures included (1) a foveal disk (1.5° radius), (2) a peripheral annulus (5° inner radius and 10° outer radius), (3) an upper vertical meridian wedge (10° radius and 60° angle), (4) a lower vertical meridian wedge (10° radius and 60° angle), (5) a left horizontal meridian wedge (10° radius and 30° angle), and (6) a right horizontal meridian wedge (10° radius and 30° angle).

The stimuli for the face/place localizer experiment were based on "full-screen" images of group photo faces and indoor laboratory scenes (10 images from each category), which were presented within a large circular aperture (10° radius), on a black background. These face and place images were qualitatively matched in visual complexity and natural image statistics (e.g., the spatial frequency distribution, the quantity of objects, and the degree of clutter), and they were successfully used in our previous studies for localizing face- and scene-selective

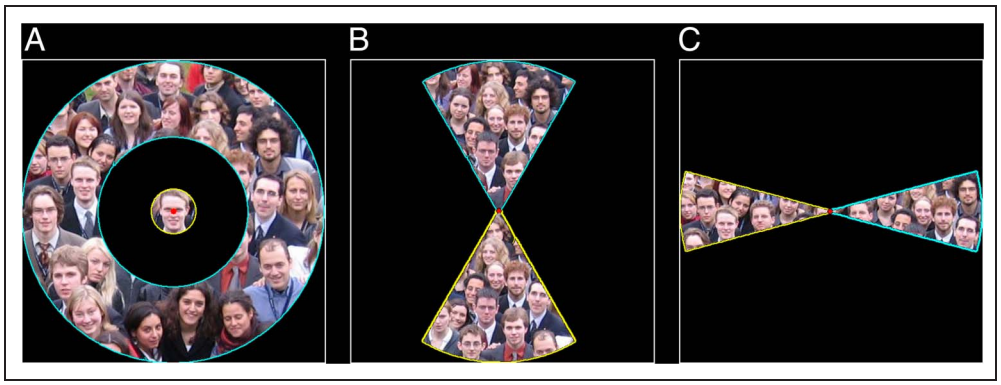

Figure 1. Stimuli used for face retinotopy in macaques. The stimuli were face-based images confined to retinotopically specific apertures. Six retinotopic conditions were tested: (A) fovea and periphery, (B) upper and lower vertical meridians, and (C) left and right horizontal meridians. The face stimuli were presented in a blocked design, with each block containing only one retinotopic condition. The white squares and yellow/cyan borders around the stimuli are for illustration purposes.

areas in humans and monkeys (Rajimehr, Devaney, Bilenko, Young, & Tootell, 2011; Rajimehr, Young, & Tootell, 2009).

All stimuli were presented in a blocked design for maximal sensitivity. Within a functional scan, the first and last blocks were null (fixation only) epochs, and the remaining stimulus blocks were ordered pseudo-randomly. Within a stimulus block, multiple examples of a particular stimulus condition (e.g., foveal disks containing face images) were randomly presented, with each image presented for 1 sec.

RESULTS

First we localized face-selective patches in the two macaque subjects, by comparing the fMRI response to faces versus places. Consistent with previous reports (Ku, Tolias, Logothetis, & Goense, 2011; Bell, Hadj-Bouziane, Frihauf, Tootell, & Ungerleider, 2009; Pinsk et al., 2009; Rajimehr et al., 2009; Tsao, Moeller, & Freiwald, 2008; Tsao, Schweers, Moeller, & Freiwald, 2008; Tsao, Freiwald, Tootell, & Livingstone, 2006; Pinsk, DeSimone, Moore, Gross, & Kastner, 2005; Tsao et al., 2003), the activity maps

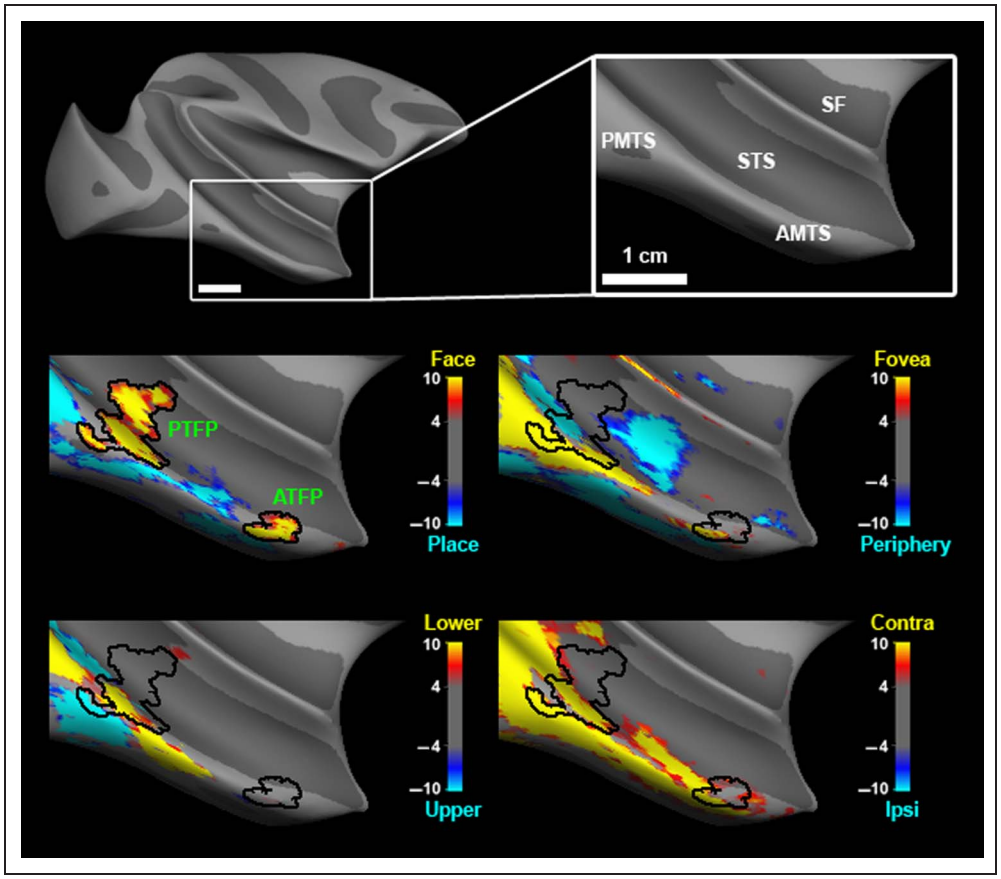

Figure 2. Topographic relationship between retinotopic maps and face patches in macaque IT cortex. The maps are displayed on an inflated view of macaque IT cortex in one hemisphere (monkey R, right hemisphere). Two major face patches in IT cortex (PTFP and ATFP) were localized based on the comparison between faces versus places. The retinotopic comparisons included the following: fovea versus periphery, upper versus lower visual fields, and contralateral versus ipsilateral visual fields. The color scale bars indicate the p values in a logarithmic format. Sulcal abbreviations: STS = superior temporal; SF = Sylvian fissure; PMTS = posterior middle temporal; AMTS = anterior middle temporal.

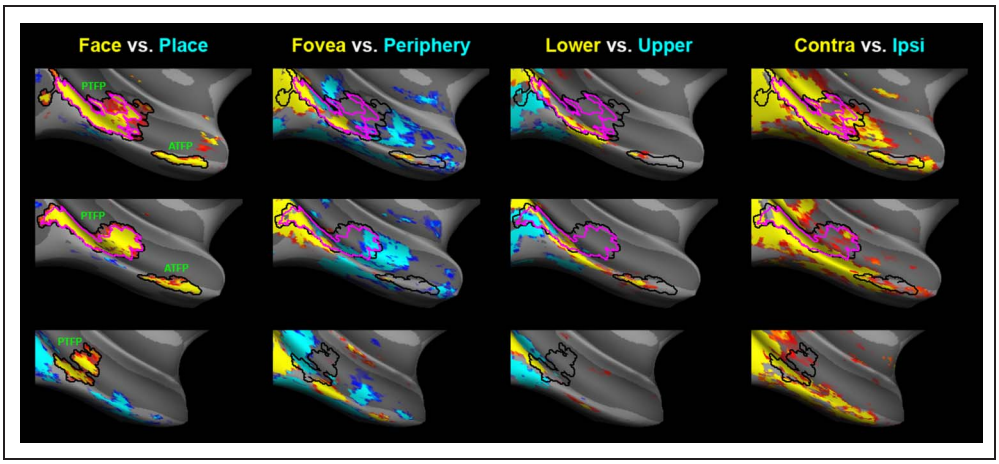

Figure 3. Additional examples of retinotopy versus face selectivity in macaque IT cortex. The face/place and retinotopic maps in IT cortex are shown for the other three hemispheres tested (map threshold: $p < 10^{-4}$ in all panels). Each row shows data from an individual hemisphere (the top row: monkey J, right hemisphere; the middle row: monkey J, left hemisphere; the bottom row: monkey R, left hemisphere). ATFP was not localized in one hemisphere (see the bottom row). PTFP was extensive in one monkey (see the top and the middle rows), and we defined its central, "hot spot" area (indicated with a purple contour) by increasing the statistical threshold ($p < 10^{-8}$) in the face/place maps.

revealed a network of face patches in monkey visual cortex. To evaluate retinotopy, here we focused on the most prominent face patches in IT and frontal cortex (i.e., the patches that were large in size and had the strongest signal; Figures 2–4). These face patches included (1) a posterior temporal face patch (PTFP), (2) an anterior temporal face patch (ATFP), and (3) a frontal face patch (FFP). In a typical macaque map, PTFP was located anterior and lateral to TEO as defined by retinotopy (Figure 5) and the cortical folding (Boussaoud et al., 1991). The IT face patches have been recently subdivided into smaller patches by Tsao et al. (Moeller, Freiwald, & Tsao, 2008; Tsao, Moeller, et al., 2008). For example, PTFP here corresponds to the two middle face patches (ML and MF) of Tsao et al. However, these subdivisions were not consistently found in our data. In addition, Tsao et al. used smaller face stimuli compared

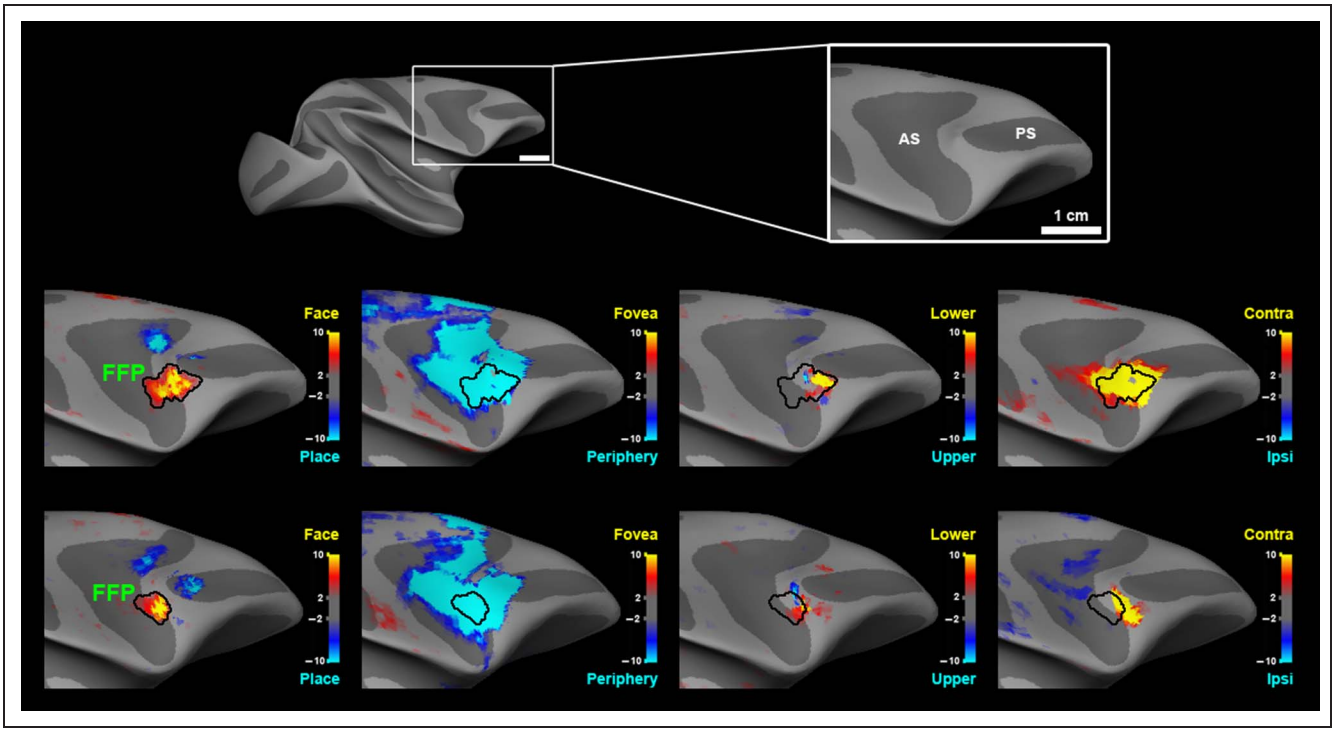

Figure 4. Topographic relationship between retinotopic maps and a face patch in macaque frontal cortex. The maps are displayed on an inflated view of macaque frontal cortex. An FFP was reliably localized in two hemispheres of one monkey, and the retinotopic maps are shown in these two hemispheres (each row corresponds to an individual hemisphere). The color scale bars indicate the p values in a logarithmic format. Sulcal abbreviations: AS = arcuate; PS = principal.

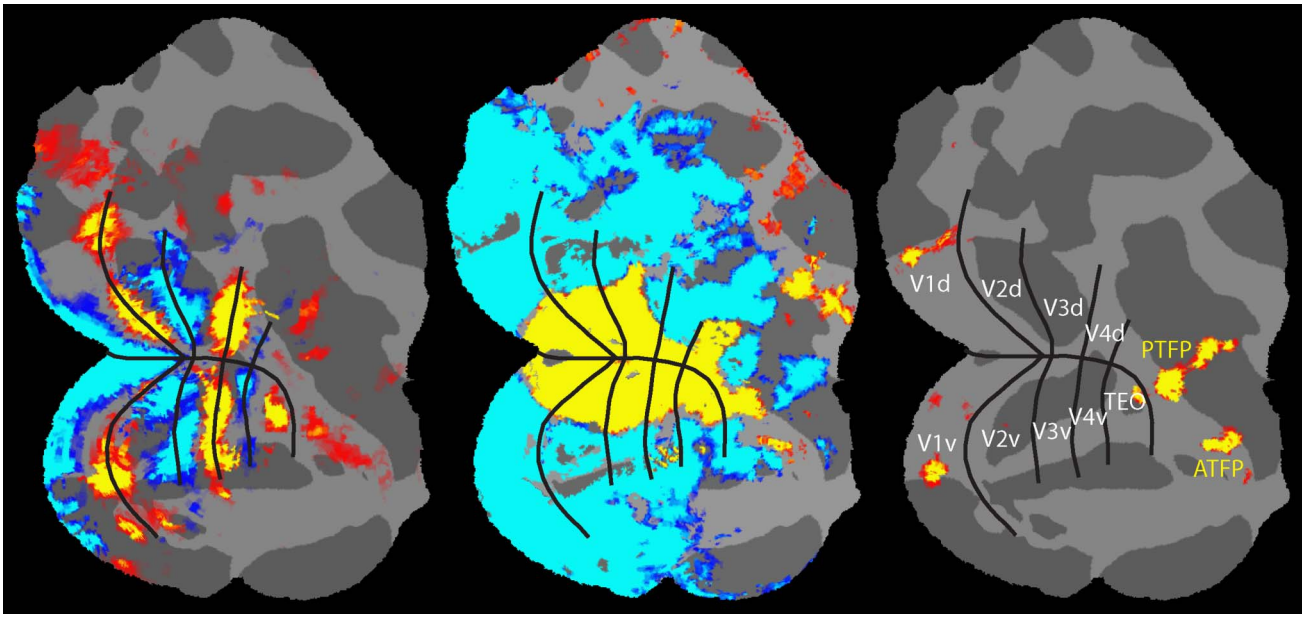

Figure 5. Location of PTFP relative to retinotopic areas. Retinotopic areas in occipital visual cortex were identified by comparing horizontal meridian (left HM + right HM) versus vertical meridian (upper VM + lower VM) stimuli. The meridian map was based on an independent set of place stimuli. This comparison revealed alternating representations of horizontal meridian (cyan) and vertical meridian (yellow), which defined the borders of V1, V2, V3, and V4. Area TEO was also identified based on an additional vertical meridian representation anterior to V4v (see Janssens, Zhu, Popivanov, & Vanduffel, in press, for a detailed retinotopic mapping of TEO and its surrounding regions). The borders of retinotopic areas are shown on an eccentricity map in the middle panel (yellow: foveal activation; cyan: peripheral activation). The map on the right is the activity map for faces versus places, showing the location of PTFP and ATFP relative to TEO and lower-tier cortical areas. The V1 activity patches in this map could be a small retinotopic artifact at the border of stimulated versus unstimulated (i.e., more peripheral) representations in V1. The map threshold is $p < 10^{-4}$. The maps are displayed on a flattened view of macaque visual cortex, in the same hemisphere shown in Figure 2.

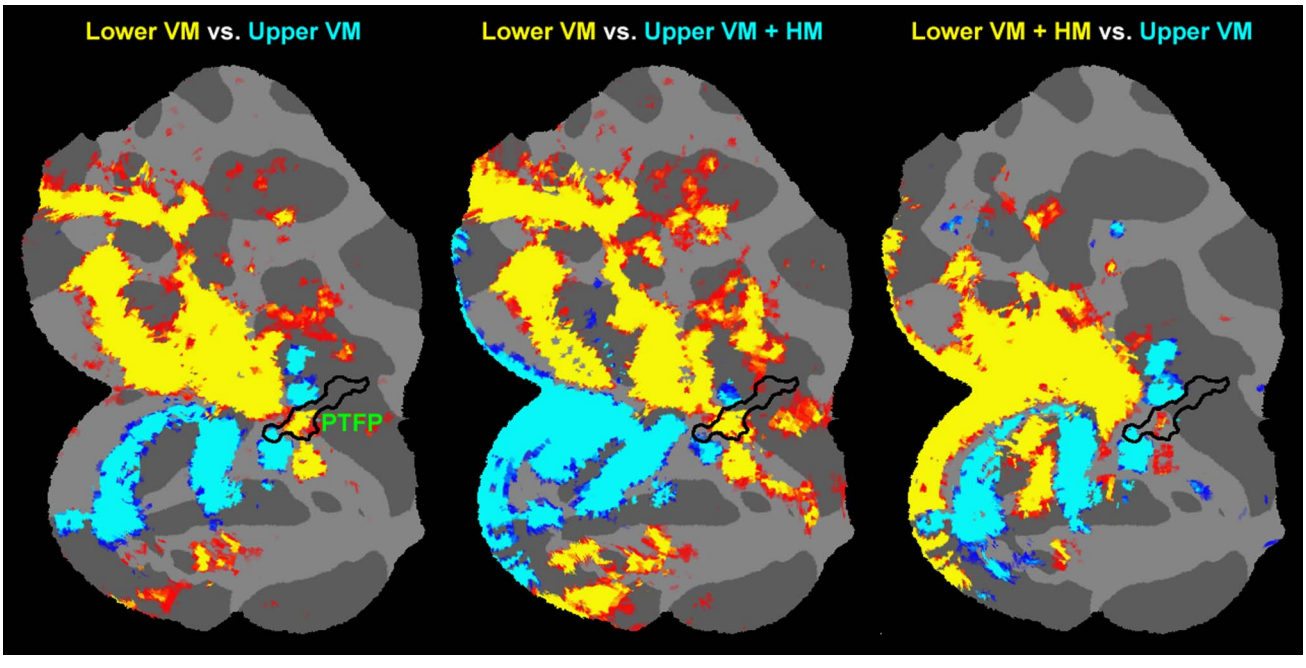

Figure 6. Additional retinotopic comparisons. The maps show activations for three contrasts: "lower VM versus upper VM," "lower VM versus upper VM + left HM + right HM," and "upper VM versus lower VM + left HM + right HM." The nonretinotopic part of PTFP within STS did not show retinotopic variation in any of the contrasts tested. The map threshold is $p < 10^{-4}$. The maps are displayed on a flattened view of macaque visual cortex in the same hemisphere shown in Figure 2.

with the stimuli used here. With spatially limited stimuli, some of the face patches may look fragmented in the fMRI maps because parts of the face patches are sensitive to the retinotopic location of faces (see below). It is also possible that the contrast used here (faces > places) showed more "face-responsive" cortex than the contrast used by Tsao et al. (faces > objects; see Bell et al., 2009 for a detailed analysis of different contrasts).

Maps of retinotopic eccentricity (fovea vs. periphery) and polar angle (upper vs. lower visual fields and contralateral vs. ipsilateral visual fields) with face stimuli revealed a heterogeneous retinotopic organization within PTFP, ATFP, and FFP (see Figures 2–4). In PTFP, the "posterior-ventral" subregion clearly showed variations in eccentricity and polar angle selectivity in all macaque hemispheres tested. In hemispheres with larger face patches, this subregion may overlap with area TEO, which has been reported to have a coarse retinotopy (Boussaoud et al., 1991). In contrast, the "anterior-dorsal" subregion of PTFP showed no retinotopic selectivity (Figure 6). The topography and size of these subregions were variable across subjects and hemispheres (see Figure 3), as described in many higher-tier retinotopic areas, and consistent with a wide individual variability in the location of areal boundaries in IT cortex (Van Essen, 2003). However in general, the fovea–periphery representation was located along the ventral–dorsal axis, and the upper–lower representation was located along the posterior–anterior axis (see Figures 2 and 3). With respect to the gyral/sulcal pattern of the cortical surface, regions along the lateral convexity of IT cortex showed more overlap between retinotopic maps and face selectivity compared with regions within the STS.

Similarly, ATFP and FFP contained subregions with retinotopic and nonretinotopic selectivity (see Figures 2–4). In some retinotopic comparisons, the retinotopic subregion was localized in the posterior part of ATFP (see Figures 2 and 3) and in the anterior part of FFP (see Figure 4). However, these face patches showed less explicit variation along a single retinotopic dimension (eccentricity or polar angle). Instead, the retinotopic subregion in these face patches had a bias to a specific location of the visual field (e.g., a small subregion in ATFP had a foveal bias; see Figure 2). Biases for eccentricity and upper or lower field also extended well outside the face patches. For instance, regions anterior to PTFP in the rostral STS showed a strong peripheral bias (see Figures 2 and 3), consistent with large and nonfoveal receptive fields in these regions (Bruce, Desimone, & Gross, 1981).

To quantify the retinotopic biases in PTFP, ATFP, and FFP, we conducted an ROI analysis (Figure 7). FFP and nearby frontal regions showed a robust peripheral bias (see also Figure 4). All face patches showed a lower visual field bias and a contralateral bias, consistent with similar retinotopic biases reported in human FFA (Schwarzlose et al., 2008; Hemond, Kanwisher, & Op de Beeck, 2007). A foveal bias has also been reported in human

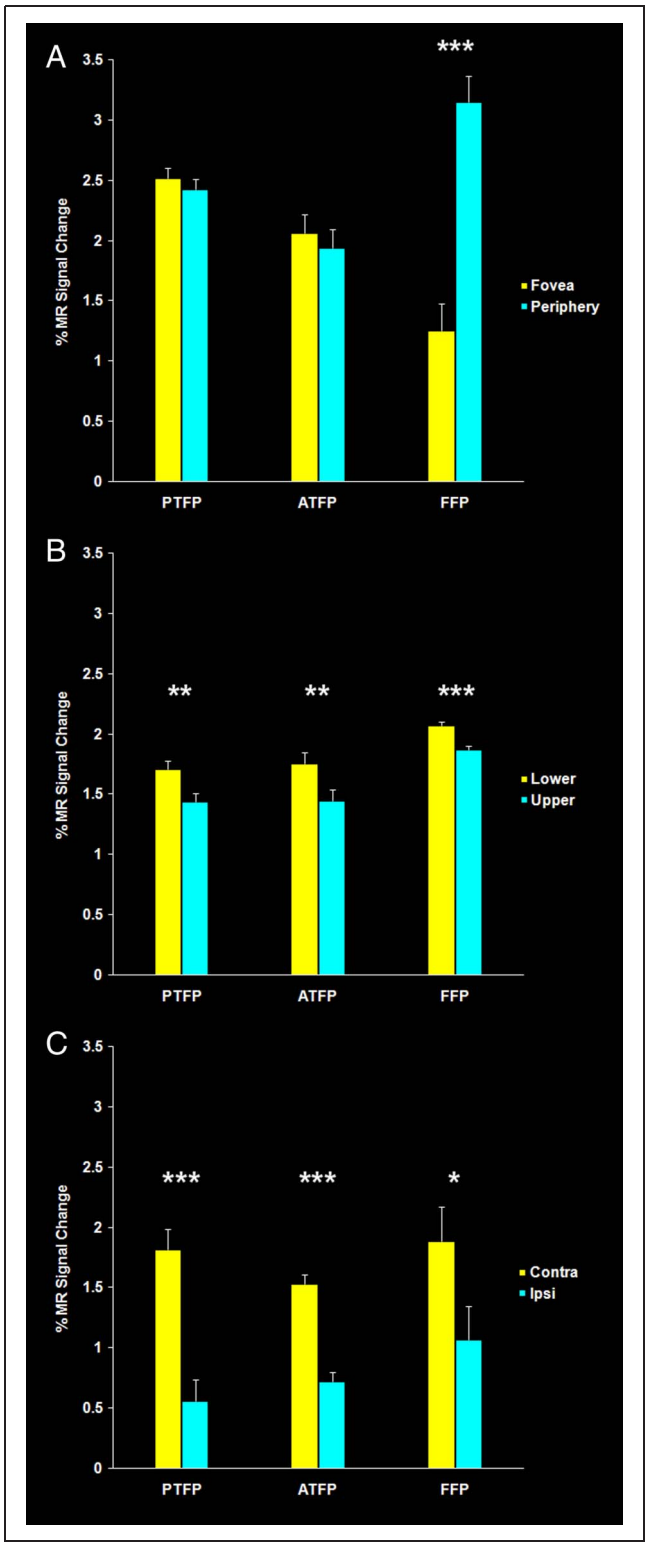

Figure 7. ROI analysis of retinotopic biases in macaque face patches. The bar plots show the fMRI activity in PTFP, ATFP, and FFP in response to faces presented in six retinotopic locations: (A) fovea and periphery, (B) upper and lower visual fields, and (C) contralateral and ipsilateral visual fields. In these plots, the fMRI responses were averaged across all hemispheres. Error bars indicate one standard error of the average. Statistical significance is denoted by asterisks (*$p < .05$; **$p < .01$; ***$p < .001$) based on paired t test. The signs of percent signal changes are known to be reversed in MION imaging compared with BOLD imaging; here those signals are inverted for convenience.

FFA (Levy et al., 2001); however, its apparent macaque homologue-PTFP (Rajimehr et al., 2009) did not show an eccentricity bias, because PTFP included distinct subregions for foveal and peripheral representations. Because of retinotopic heterogeneity within face patches, we plotted the distribution of voxels' retinotopic selectivity in all face patches (Figure 8). Consistent with the ROI analysis, a voxel-wise analysis showed no correlation between face selectivity and eccentricity bias in PTFP (Figure 9). Interestingly, there was a positive correlation between face selectivity and eccentricity bias in ATFP (more foveal bias in more selective face voxels; Figure 9). As expected from the ROI analysis, there was a strong negative correlation between face selectivity and eccentricity bias in FFP (more peripheral bias in more selective face voxels; Figure 9).

DISCUSSION

Previous fMRI studies have often distinguished "nonretinotopic" face-selective cortex from immediately adjacent "retinotopic" regions (e.g., Halgren et al., 1999). In contrast, the macaque data here strongly support a gradual/continuous rather than an abrupt transition from retinotopy to face selectivity at increasingly higher-tier levels of the ventral visual pathway. In fact, this transition appears within face-selective regions. For instance, a nonretinotopic subregion within PTFP (the largest face patch in macaques) was located adjacent to another subregion that was explicitly retinotopic. Overall, our data suggest that the ventral visual pathway contains information about faces as an object category as well as information about the spatial location of faces.

To localize the face patches, we contrasted group photographs of faces versus indoor scenes. Although it is used less frequently, this localizer has several advantages over other localizers such as "single face versus object" or "single face versus place." The group photo faces and indoor scenes were closely matched in terms of the spatial frequency distribution and other low-level image statistics. Moreover, these stimuli could be presented within a single common retinotopic aperture. In other localizers

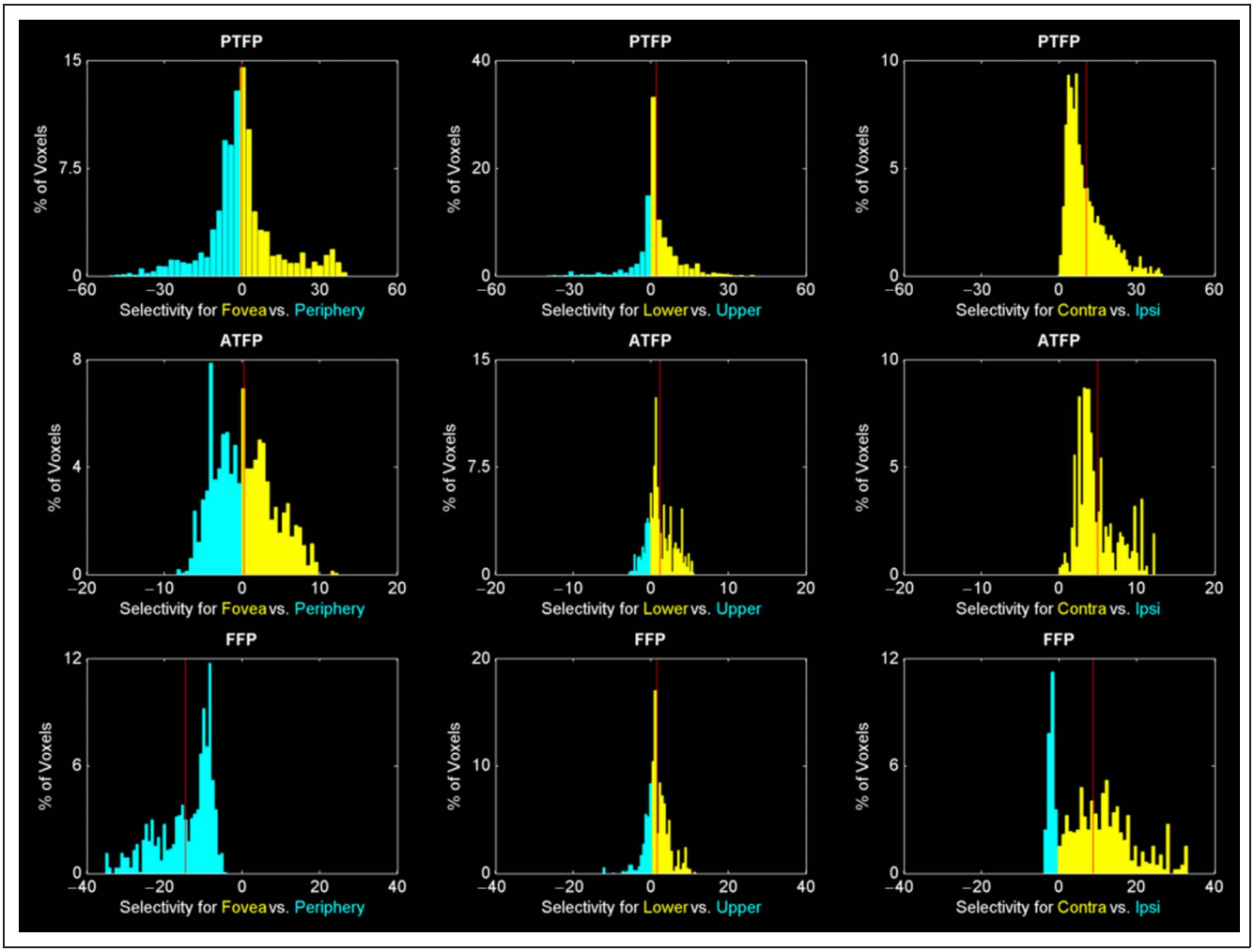

Figure 8. Distribution of retinotopic selectivity across voxels in macaque face patches. The histograms show the distribution of retinotopic selectivity in PTFP, ATFP, and FFP. In a given retinotopic comparison, the retinotopic selectivity was defined for all face-selective voxels using the "d-prime" index. All face voxels from all hemispheres are included in these histograms. In each plot, the red line indicates the mean of the distribution.

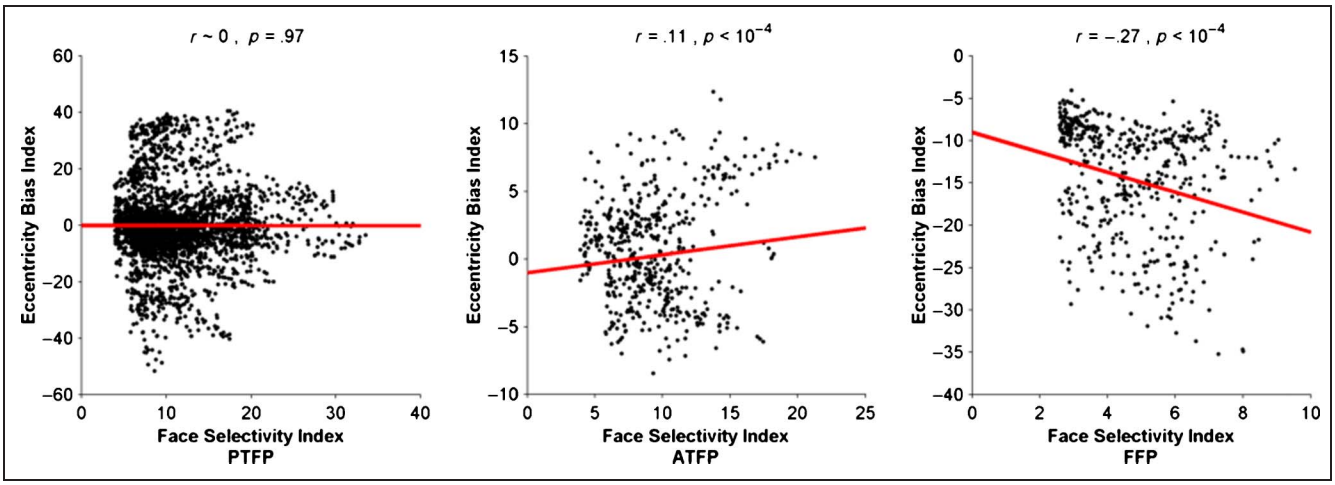

Figure 9. Correlation between face selectivity and eccentricity bias in macaque face patches. In each voxel within a face patch, face selectivity and eccentricity bias were computed using the "d-prime" index. For face selectivity, the d-prime index was defined as the discriminability of response to faces versus places. For eccentricity bias, the d-prime index was defined as the discriminability of response to foveal versus peripheral face stimuli. All face voxels from all hemispheres are shown in these scatterplots. Red lines are linear regression lines fitted to the data. Pearson's correlation coefficient (r) and its significance were calculated in each scatterplot.

(e.g., single faces vs. objects/places), the retinotopic envelopes of the stimuli are different, which could induce significant retinotopic artifacts in the maps.

To increase the statistical power in the monkey fMRI setting, we used only a few retinotopic conditions in a blocked-design experiment. However, this method can only reveal a coarse version of a retinotopic map. The face patches may contain a finer retinotopic organization if they are mapped with more detailed (e.g., phase-encoded) retinotopic stimuli.

Parts of the face patches did not show any retinotopic selectivity. However, the absence of a retinotopic map does not necessarily mean the absence of positional information. Positional information could still be present in a distributed form. Further studies are needed to assess the role of "nonretinotopic" positional information in the spatial coding of faces.

FFP and surrounding regions in pFC showed a strong peripheral bias. One possibility is that these regions have an overrepresentation of peripheral visual field (Ungerleider, Galkin, Desimone, & Gattass, 2008), and FFP is actually involved in detecting faces in the periphery. Given the proximity of FFP and FEF, peripheral coding of faces in FFP could be useful for planning eye movements toward faces in the visual field. Alternatively, the peripheral bias in FFP may simply reflect the lack of cortical magnification of fovea in this region. Because the size of our stimuli was scaled according to the cortical magnification of fovea in the ventral visual pathway, larger stimuli in the periphery would produce a larger response in FFP.

Given our macaque data, one might expect a spatial heterogeneity in the retinotopic organization within corresponding human face-selective areas (e.g., FFA). However, previous studies in humans have only reported a foveal bias in FFA and other occipitotemporal face areas (Hasson et al., 2003; Levy et al., 2001), not the more explicit retinotopy found here. The lack of more detailed retinotopy in human FFA may arise from either or both of two factors. First, it could reflect genuine species differences between macaques and humans. Some species differences have been found in previous comparisons of visual cortex in these two species (Sereno & Tootell, 2005). Second, the difference could arise as a result of technical differences between this and previous fMRI studies. Specifically, previous human fMRI experiments were based on functional images with lower spatial resolution compared with the spatial resolution used in the monkey fMRI experiments here (voxel size = 1.25 mm isotropic). Moreover, it is known that MION imaging (used in the monkeys) is more specific for gray matter compared with BOLD imaging in humans (Leite et al., 2002). Because some behavioral studies have shown evidence for position-dependent face perception in humans (e.g., Afraz, Pashkam, & Cavanagh, 2010; Afraz & Cavanagh, 2008), it is conceivable that further increases in fMRI sensitivity will reveal subtler variations in retinotopy, even in human face-selective areas.

Finally our data on retinotopy in IT cortex could be used in assessing homologies between macaque and human face-selective areas. Previous studies have suggested that the macaque PTFP is the homologue of the human FFA (e.g., Rajimehr et al., 2009). PTFP often shows two "hot spots" of face selectivity (see Figure 2), which are named ML (middle lateral) and MF (middle fundus) by Tsao, Moeller, et al. (2008). ML or the lateral part of PTFP showed foveal selectivity, similar to a foveal bias in human FFA. This suggests that ML is a putative homologue of the foveal region in FFA.

Acknowledgments

We thank Leeland Ekstrom for help with the monkey fMRI and two anonymous reviewers for comments on this manuscript. This research was supported by the National Institutes of Health

(grants R01 MH67529 and R01 EY017081 to R. B. H. T.), the Martinos Center for Biomedical Imaging, the NCRR, and the MIND Institute.

Reprint requests should be sent to Reza Rajimehr, NMR Martinos Center, Massachusetts General Hospital (MGH), 149 Thirteenth Street, Room 2301, Charlestown, MA 02129, or via e-mail: reza@nmr.mgh.harvard.edu.

REFERENCES

Afraz, A., Pashkam, M. V., & Cavanagh, P. (2010). Spatial heterogeneity in the perception of face and form attributes. *Current Biology, 20,* 2112–2116.

Afraz, S. R., & Cavanagh, P. (2008). Retinotopy of the face aftereffect. *Vision Research, 48,* 42–54.

Arcaro, M. J., McMains, S. A., Singer, B. D., & Kastner, S. (2009). Retinotopic organization of human ventral visual cortex. *Journal of Neuroscience, 29,* 10638–10652.

Bell, A. H., Hadj-Bouziane, F., Frihauf, J. B., Tootell, R. B., & Ungerleider, L. G. (2009). Object representations in the temporal cortex of monkeys and humans as revealed by functional magnetic resonance imaging. *Journal of Neurophysiology, 101,* 688–700.

Boussaoud, D., Desimone, R., & Ungerleider, L. G. (1991). Visual topography of area TEO in the macaque. *Journal of Comparative Neurology, 306,* 554–575.

Brewer, A. A., Liu, J., Wade, A. R., & Wandell, B. A. (2005). Visual field maps and stimulus selectivity in human ventral occipital cortex. *Nature Neuroscience, 8,* 1102–1109.

Brewer, A. A., Press, W. A., Logothetis, N. K., & Wandell, B. A. (2002). Visual areas in macaque cortex measured using functional magnetic resonance imaging. *Journal of Neuroscience, 22,* 10416–10426.

Bruce, C., Desimone, R., & Gross, C. G. (1981). Visual properties of neurons in a polysensory area in superior temporal sulcus of the macaque. *Journal of Neurophysiology, 46,* 369–384.

Carlson, T., Hogendoorn, H., Fonteijn, H., & Verstraten, F. A. (2011). Spatial coding and invariance in object-selective cortex. *Cortex, 47,* 14–22.

Cichy, R. M., Chen, Y., & Haynes, J. D. (2011). Encoding the identity and location of objects in human LOC. *Neuroimage, 54,* 2297–2307.

DeYoe, E. A., Carman, G. J., Bandettini, P., Glickman, S., Wieser, J., Cox, R., et al. (1996). Mapping striate and extrastriate visual areas in human cerebral cortex. *Proceedings of the National Academy of Sciences, U.S.A., 93,* 2382–2386.

DiCarlo, J. J., & Maunsell, J. H. (2003). Anterior inferotemporal neurons of monkeys engaged in object recognition can be highly sensitive to object retinal position. *Journal of Neurophysiology, 89,* 3264–3278.

Engel, S. A., Rumelhart, D. E., Wandell, B. A., Lee, A. T., Glover, G. H., Chichilnisky, E. J., et al. (1994). fMRI of human visual cortex. *Nature, 369,* 525.

Felleman, D. J., & Van Essen, D. C. (1991). Distributed hierarchical processing in the primate cerebral cortex. *Cerebral Cortex, 1,* 1–47.

Fize, D., Vanduffel, W., Nelissen, K., Denys, K., Chef d'Hotel, C., Faugeras, O., et al. (2003). The retinotopic organization of primate dorsal V4 and surrounding areas: A functional magnetic resonance imaging study in awake monkeys. *Journal of Neuroscience, 23,* 7395–7406.

Gattass, R., Sousa, A. P., & Gross, C. G. (1988). Visuotopic organization and extent of V3 and V4 of the macaque. *Journal of Neuroscience, 8,* 1831–1845.

Halgren, E., Dale, A. M., Sereno, M. I., Tootell, R. B., Marinkovic, K., & Rosen, B. R. (1999). Location of human face-selective cortex with respect to retinotopic areas. *Human Brain Mapping, 7,* 29–37.

Hasson, U., Harel, M., Levy, I., & Malach, R. (2003). Large-scale mirror-symmetry organization of human occipito-temporal object areas. *Neuron, 37,* 1027–1041.

Hemond, C. C., Kanwisher, N. G., & Op de Beeck, H. P. (2007). A preference for contralateral stimuli in human object- and face-selective cortex. *PLoS One, 2,* e574.

Janssens, T., Zhu, Q., Popivanov, I. D., & Vanduffel, W. (in press). Probabilistic and single-subject retinotopic maps reveal the topographic organization of face patches in the macaque cortex.

Kanwisher, N., McDermott, J., & Chun, M. M. (1997). The fusiform face area: A module in human extrastriate cortex specialized for face perception. *Journal of Neuroscience, 17,* 4302–4311.

Kravitz, D. J., Kriegeskorte, N., & Baker, C. I. (2010). High-level visual object representations are constrained by position. *Cerebral Cortex, 20,* 2916–2925.

Kravitz, D. J., Vinson, L. D., & Baker, C. I. (2008). How position dependent is visual object recognition? *Trends in Cognitive Sciences, 12,* 114–122.

Ku, S. P., Tolias, A. S., Logothetis, N. K., & Goense, J. (2011). fMRI of the face-processing network in the ventral temporal lobe of awake and anesthetized macaques. *Neuron, 70,* 352–362.

Larsson, J., & Heeger, D. J. (2006). Two retinotopic visual areas in human lateral occipital cortex. *Journal of Neuroscience, 26,* 13128–13142.

Leite, F. P., Tsao, D., Vanduffel, W., Fize, D., Sasaki, Y., Wald, L. L., et al. (2002). Repeated fMRI using iron oxide contrast agent in awake, behaving macaques at 3 Tesla. *Neuroimage, 16,* 283–294.

Levy, I., Hasson, U., Avidan, G., Hendler, T., & Malach, R. (2001). Center-periphery organization of human object areas. *Nature Neuroscience, 4,* 533–539.

Malach, R., Levy, I., & Hasson, U. (2002). The topography of high-order human object areas. *Trends in Cognitive Sciences, 6,* 176–184.

Moeller, S., Freiwald, W. A., & Tsao, D. Y. (2008). Patches with links: A unified system for processing faces in the macaque temporal lobe. *Science, 320,* 1355–1359.

Op De Beeck, H., & Vogels, R. (2000). Spatial sensitivity of macaque inferior temporal neurons. *Journal of Comparative Neurology, 426,* 505–518.

Pinsk, M. A., Arcaro, M., Weiner, K. S., Kalkus, J. F., Inati, S. J., Gross, C. G., et al. (2009). Neural representations of faces and body parts in macaque and human cortex: A comparative fMRI study. *Journal of Neurophysiology, 101,* 2581–2600.

Pinsk, M. A., DeSimone, K., Moore, T., Gross, C. G., & Kastner, S. (2005). Representations of faces and body parts in macaque temporal cortex: A functional MRI study. *Proceedings of the National Academy of Sciences, U.S.A., 102,* 6996–7001.

Porat, Y., Pertzov, Y., & Zohary, E. (2011). Viewed actions are mapped in retinotopic coordinates in the human visual pathways. *Journal of Vision, 11,* 17.

Rajimehr, R., Devaney, K. J., Bilenko, N. Y., Young, J. C., & Tootell, R. B. (2011). The "parahippocampal place area" responds preferentially to high spatial frequencies in humans and monkeys. *PLoS Biology, 9,* e1000608.

Rajimehr, R., Young, J. C., & Tootell, R. B. (2009). An anterior temporal face patch in human cortex, predicted by macaque maps. *Proceedings of the National Academy of Sciences, U.S.A., 106,* 1995–2000.

Sayres, R., & Grill-Spector, K. (2008). Relating retinotopic and object-selective responses in human lateral occipital cortex. *Journal of Neurophysiology, 100,* 249–267.

Schwarzlose, R. F., Swisher, J. D., Dang, S., & Kanwisher, N. (2008). The distribution of category and location information

across object-selective regions in human visual cortex. *Proceedings of the National Academy of Sciences, U.S.A., 105,* 4447–4452.

Sereno, M. I., Dale, A. M., Reppas, J. B., Kwong, K. K., Belliveau, J. W., Brady, T. J., et al. (1995). Borders of multiple visual areas in humans revealed by functional magnetic resonance imaging. *Science, 268,* 889–893.

Sereno, M. I., & Tootell, R. B. (2005). From monkeys to humans: What do we now know about brain homologies? *Current Opinion in Neurobiology, 15,* 135–144.

Strother, L., Aldcroft, A., Lavell, C., & Vilis, T. (2010). Equal degrees of object selectivity for upper and lower visual field stimuli. *Journal of Neurophysiology, 104,* 2075–2081.

Tsao, D. Y., Freiwald, W. A., Knutsen, T. A., Mandeville, J. B., & Tootell, R. B. (2003). Faces and objects in macaque cerebral cortex. *Nature Neuroscience, 6,* 989–995.

Tsao, D. Y., Freiwald, W. A., Tootell, R. B., & Livingstone, M. S. (2006). A cortical region consisting entirely of face-selective cells. *Science, 311,* 670–674.

Tsao, D. Y., Moeller, S., & Freiwald, W. A. (2008). Comparing face patch systems in macaques and humans. *Proceedings of the National Academy of Sciences, U.S.A., 105,* 19514–19519.

Tsao, D. Y., Schweers, N., Moeller, S., & Freiwald, W. A. (2008). Patches of face-selective cortex in the macaque frontal lobe. *Nature Neuroscience, 11,* 877–879.

Ungerleider, L. G., & Desimone, R. (1986). Cortical connections of visual area MT in the macaque. *Journal of Comparative Neurology, 248,* 190–222.

Ungerleider, L. G., Galkin, T. W., Desimone, R., & Gattass, R. (2008). Cortical connections of area V4 in the macaque. *Cerebral Cortex, 18,* 477–499.

Van Essen, D. C. (2003). Organization of visual areas in macaque and human cerebral cortex. In L. Chalupa & J. S. Werner (Eds.), *The visual neurosciences* (pp. 507–521). Cambridge, MA: MIT Press.

Vanduffel, W., Fize, D., Mandeville, J. B., Nelissen, K., Van Hecke, P., Rosen, B. R., et al. (2001). Visual motion processing investigated using contrast agent-enhanced fMRI in awake behaving monkeys. *Neuron, 32,* 565–577.

Weiner, K. S., & Grill-Spector, K. (2011). Not one extrastriate body area: Using anatomical landmarks, hMT+, and visual field maps to parcellate limb-selective activations in human lateral occipitotemporal cortex. *Neuroimage, 56,* 2183–2199.